Radiation Distribution Sensing with Normal Optical Fiber

R. Naka[1], J. Kawarabayashi[1], A. Uritani[1], T. Iguchi[1],
J. Kaneko[2], H. Takeuchi[2] and T. Kakuta[2]

[1]Department of Nuclear Engineering, School of Engineering, Nagoya University
Furo-cho, Chikusa-ku, Nagoya, 464-8603, Japan
[2]Japan Atomic Energy Research Institute (JAERI)
Tokai-mura, Ibaraki-ken, 319-1195, Japan

Abstract

The purpose of this study is to develop a radiation distribution monitor using a normal plastic optical fiber. The monitor has a long operating length and can obtain continuous radiation distributions. A principle of the position sensing is based on a time-of-flight technique. The monitor is sensitive to beta rays or charged particles, gamma rays, and fast neutrons. The spatial resolutions for beta rays (^{90}Sr-^{90}Y), gamma rays (^{137}Cs) and D-T neutrons are 30 cm, 37 cm and 13 cm, respectively. The detection efficiencies for the beta rays, the gamma rays and D-T neutrons are 0.11%, 1.6x10^{-5}% and 1.2x10^{-4}%, respectively. The effective attenuation length of the detection efficiency is 18m. In this paper, we describe the basic characteristics of this monitor.

I. INTRODUCTION

There is a demand of a new radiation distribution monitor that can be used around nuclear reactors, nuclear fusion experimental devices, accelerators and so on. The monitor should have three characteristics, i.e. a long operation length, a continuous sensitivity and real time operation.

Recently, some methods [1] of radiation distribution sensing with optical fibers have been proposed. These methods employ a scintillating fiber [2], or scintillators with wavelength-shifting fibers [3]. In the former method, the attenuation length for the scintillation photons in the scintillating fiber is relatively short, so that the operating length of the sensor is limited to a few meters. In the latter method, the sensor cannot obtain a continuous radiation distribution but discrete one.

To improve these shortcomings, we propose a new method using a normal plastic optical fiber (POF) made of polymethylmethacrylate (PMMA). The new radiation monitor has major advantages, such as a long operation length, continuous sensitivity, real time operation, insensitivity to electromagnetic fields and a simple measuring system. We describe the characteristics of the radiation distribution monitor using the POF.

II. PRINCIPLE AND SETUP

Figure 1 shows the conceptual diagram of this position-sensing method. The time-of-flight technique (TOF) was used to detect positions of radiation interactions. When a radiation enters and interacts with the POF, fluorescent and/or Cherenkov lights are emitted. When enough amounts of the photons are emitted within the critical angle of the POF and the photons reach both ends of the POF, the position of radiation interaction can be detected. When the photons reach both ends of the POF, we can obtain the following simple expression.

$$X = C'(T_1 - T_2)/2 ,$$

where X is the distance between the position of radiation interaction and the left end of the POF, C' is the velocity of light in PMMA, T_1 and T_2 are time durations with which the photons reach the left and the right ends, respectively. Figure 2 shows the block diagram of the measuring system. The length of the POF (MITSUBISHI RAYON SH8001, Step index mode : multi mode) was 10m to 100m and the diameter was 2mm. A photomultiplier tube (PMT Hamamatsu-Photonics R1635) followed by a fast pre-amplifier (ORTEC EG&G VT120) and a constant fraction discriminator (CFD) was connected to each end of the POF. The output signals of the POF were fed to a time-to-amplitude converter (TAC). The output pulse heights of the TAC were analyzed with a multi-channel analyzer (MCA). A delay amplifier gave an appropriate delay time.

Position of radiation interaction

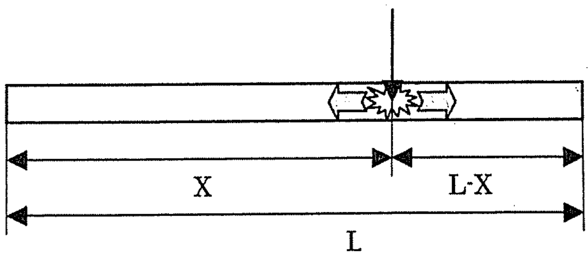

Figure 1: Conceptual diagram of the position sensing method.

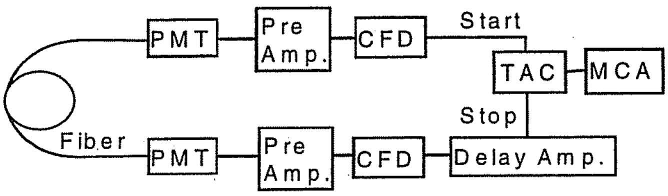

Figure 2: The block diagram of the system.

0-7803-6503-8/01/$10.00 2001 IEEE

III. Experimental Results

A. Response to Beta Rays

A ^{90}Sr-^{90}Y beta source with an activity of 14kBq was used. A cylindrical collimator with an inner diameter of 4.5mm collimated the beta particles. The length of the POF was 10m. The spatial resolution (FWHM) was 30cm. The intrinsic detection efficiency was 0.11%.

B. Response to Gamma Rays

A ^{137}Cs gamma-ray source with an activity of 54.2MBq was used. A divergent collimator with inlet and outlet aperture diameters of 8mm and 55mm, respectively, and with a length of 40mm was used. The POF was placed at the outlet aperture of the collimator. The length of the POF was 10m. The spatial resolution was 37cm. The intrinsic detection efficiency was 1.6×10^{-5}%.

C. Response to Fission Neutrons

A fission neutron beam at the Yayoi [4] that was a fast neutron reactor was used. The neutron beam was collimated to 50mm in diameter. The average energy was 1.3MeV. The flux and the fluence were 4.5×10^{6} n/cm²·s and 8.1×10^{9} n/cm², respectively. The length of the POF was 10m. The spatial resolution was 33cm. The intrinsic detection efficiency was 2.0×10^{-5}%.

D. Response to D-T Neutrons

A D-T neutron beam at the Fusion Neutronics Source [5] (FNS), in JAERI, was used. The neutron beam was collimated to 20 mm in diameter. The length of the POF was 10m. Figure 3 shows the results of the neutron measurements with and without a polyethylene shield with a thickness of 40cm that was placed in front of the POF. The flux was 1.2×10^{6} n/cm²·s. The fluence was 7.2×10^{8} n/cm². The spatial resolution was 13cm. The intrinsic detection efficiency was 5.4×10^{-4}%.

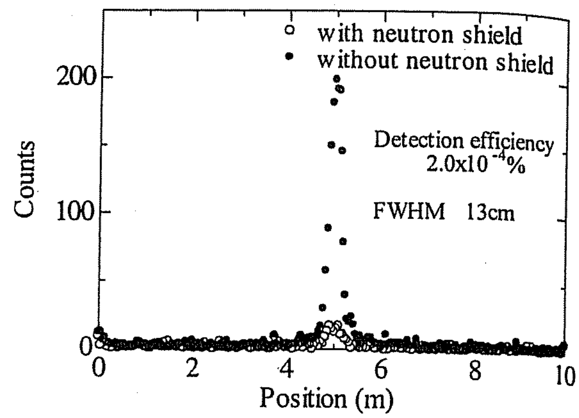

Figure 3: The response to the D-T neutrons.

E. Measurements with Longer POFs

1) Measurement with the 20m POF

The 20m POF was used for the first step to develop a longer detector. The fission neutron beam at the Yayoi was used. The POF was irradiated by the neutrons at four different points to evaluate the position dependency of the detection efficiency and the spatial resolution. Figure 4 shows the experimental results. The flux was 9.0×10^{6} n/cm²·s. The fluence was 5.4×10^{9} n/cm². The spatial resolution was 42cm. The intrinsic detection efficiency was 1.7×10^{-5}%. The intrinsic detection efficiency and the spatial resolution were worse than those obtained with the 10m POF. No position dependency of these characteristics was observed. The ^{90}Sr-^{90}Y beta source was also used. The spatial resolution was 46cm. The intrinsic detection efficiency was 2.3×10^{-4}%.

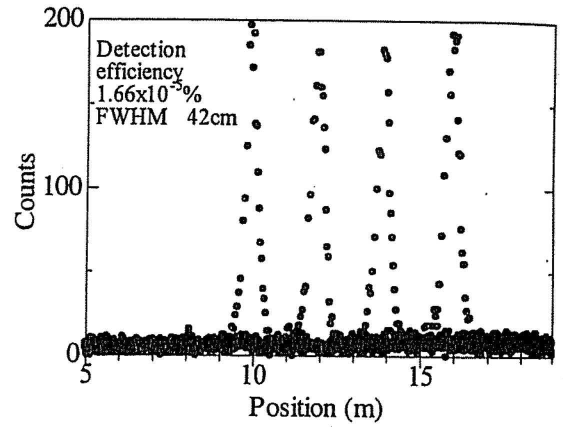

Figure 4: The response to fast neutron at Yayoi (20m fiber).

2) Measurements with the 50m POF

The D-T neutron beam at the FNS was used. Figure 5 shows the result obtained with the 50m POF. The flux was 2.4×10^{5} n/cm²·s. The fluence was 1.0×10^{9} n/cm². The spatial resolution was 90cm. The intrinsic detection efficiency was 2.5×10^{-5}%.

3) Measurements with the 100m POF

The D-T neutron beam at the FNS was used. The length of the POF was 100m. The flux was 2.2×10^{5} n/cm²·s. The fluence was 3.1×10^{9} n/cm². The spatial resolution was 2.5m. The intrinsic detection efficiency was 4.3×10^{-6}%.

F. Optical property of POF

We investigated the emission light spectrum at the ^{60}Co irradiation facility in JAERI to know the optical characteristics of the POF.

1) Emission Spectrum

A jointed fiber composed the POF with a length of 30cm as an irradiation part and a quartz fiber as a transmission part was used. Figure 6 shows the emission spectrum of the POF irradiated by ^{60}Co gamma rays. The yield of Cherenkov photons per unit wavelength λ is proportional to $1/\lambda^2$. The emission is concerned in the short-wavelength region of the spectrum. The Cherenkov glow component was therefore dominant in the spectrum. However, the scintillating light existed in wavelength region of 600 to 800nm, and even in 400 to 600nm region.

2) Radiation Damage

The emission spectra were measured to investigate radiation damages of the POF. Here both the irradiation and the transmission part is the POF. Figure 7 shows the result. Some optical absorption by the POF existed before and after the irradiation. The absorptions at 530nm, 620nm and 730nm were due to the inherent optical absorption property of the POF. The light yield between 300nm and 600nm decreased by absorption due to radiation damage. The light components above 600nm were not influenced by the irradiation.

G. Ratio of Foreground Events to Total Events

Only a small fraction of total scintillating events can be detected as the foreground events in this measurement, because the small number of photons produced upon a radiation interaction cannot reach both ends of the POF due to the transmission property and a directional property of Cherenkov emission. We evaluated the fraction of the foreground events to the total one. The number of the total events was obtained as the number of events that the photons reach the photocathode of the PMT, when the ^{90}Sr-^{90}Y beta source is placed at 5cm from the PMT. The number of the detected events as position signals, namely foreground events was obtained when the beta source was placed at 7m from the end of the POF with a length of 10m. Figure 8 shows the result. The fraction of the foreground to the total events was 0.4%. Most of the total events were the Cherenkov glows. Since Cherenkov photons had directional property, they seldom satisfy the detectable condition. Some of the backgrounds were chance coincidence events of the Cherenkov photons.

IV. Discussion

A. Spatial Resolution

We calculated the expansion of a transmission time of photons by taking the mode dispersion of the POF into consideration. The fastest photons have no reflection during transmission before reaching the end of the POF, if the POF is straight. The slowest photons have much reflection during transmission along the path with the critical angle. The difference between the fastest and the slowest accession times, τ, is given by the following equations.

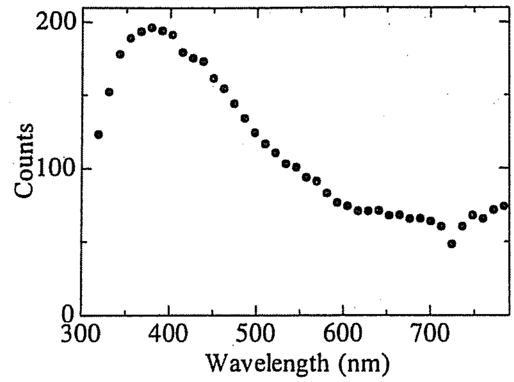

Figure 6: The spectrum of the light emitted in jointed fiber.

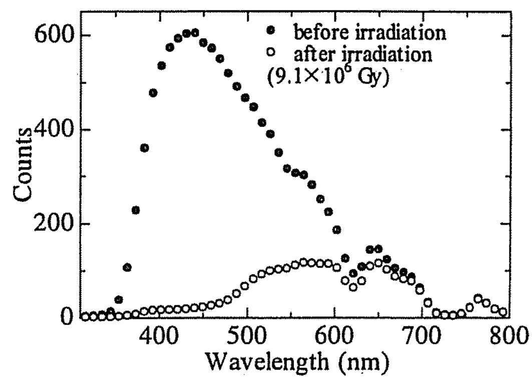

Figure 7: The spectrum of the light emitted in the POF.

$$\tau = \frac{n_1 \Delta}{c} L,$$

$$\Delta = \frac{n_1^2 - n_2^2}{2n_1^2} \approx \frac{n_1 - n_2}{n_1},$$

where n_1 and n_2 are the refractive indexes of the core (1.495) and the clad (1.402), and c is the velocity of light in vacuum. For example, we set one of the difference times as τ_1, and the other τ_2. Since both sides of the POF are used, the maximum difference time is $\tau_1+\tau_2$. When the 50 m POF was irradiated at 40 m point, the difference times, τ_1 and τ_2 are 12ns and 3ns, respectively. The maximum difference time, $\tau_1+\tau_2$, is 15ns, which corresponds to 1.4m. As described before, the experimentally obtained FWHM and FWTM of the 50m POF were 0.90m and 1.80m, respectively. Therefore the dominant factor that determines the spatial resolution is this time difference.

This detector has better spatial resolution for the D-T neutrons than for other radiations. In comparison with electrons, the energy deposit by a recoil proton is large. A 10MeV recoil proton can deposit the full energy. On the other hand, a 1MeV electron can deposited 400keV at most. Approximately, the energy deposited is different about 30 times. Considering the yield of a light emission property of organic scintillators, the yield of the emission light by the recoil proton is roughly estimated to be about 10 times lager than that by the electron. Since the large yield of the emission light for the D-T neutrons reduced fluctuations due to jitters and walks, the spatial resolution was relatively good.

B. Effective Attenuation Length for Detection Efficiency

When a radiation interacts with the POF and the photons are emitted at X in Figure 1, the probability P_L that the photons reach the left end of the POF is expressed as $P_L=A\exp(-\mu X)$, where A is an appropriate constant value determined by the geometrical condition of the POF and μ is the effective attenuation constant for the photons. Similarly $P_R=A\exp[-\mu(L-X)]$. Hence the probability P that the photons reach both ends of the POF is expressed as

$$P = P_L P_R = A^2 \exp(-\mu L)$$

Therefore the detection efficiency depends on the length of the POF. We treated the μ as an effective attenuation constant value although it depends on the wavelength or the reflection angle. We measured the detection efficiency with the POF with four different lengths of 10m, 20m, 50m and 100m to obtain the effective attenuation constant. The four detection efficiencies were fitted by the exponential function. The attenuation length, $1/\mu$, of the POF was 18m.

C. Emission Spectrum

Since Cherenkov photons have the directional property, Cherenkov photons seldom satisfy the detectable condition. Therefore the foreground signals were only 0.4% of the total event numbers. This detector can measure recoil protons produced by fast neutrons. We need to measure the wavelength spectrum of the emission light produced by the protons that are recoiled fast neutrons because D-T neutrons and the recoil protons never generate the Cherenkov photons.

V. CONCLUSION

We have developed a radiation distribution monitor using the POF for long, complicated, and narrow spaces. The responses of this monitor to the several radiations have been studied. We estimated the major factor of the spatial resolution. We obtained the effective attenuation length of the detection efficiencies.

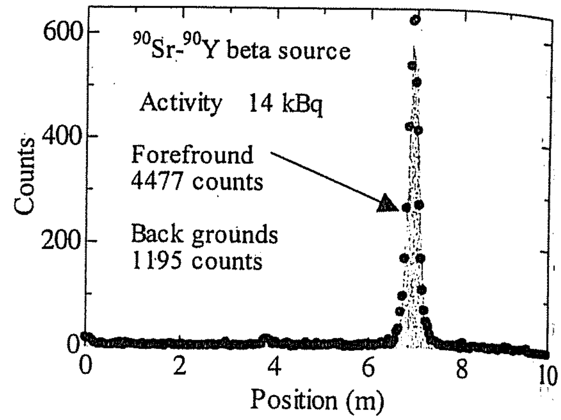

Figure 8: The ratio of foreground signals.

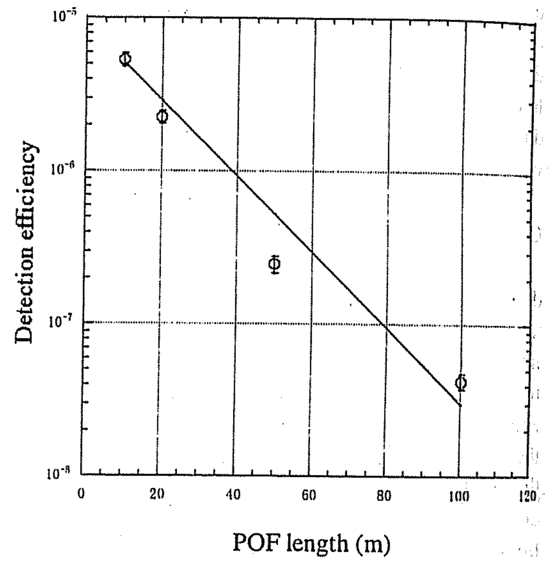

Figure 9: The graph of the detection efficiencies to estimate the attenuation length.

VI. REFERENCES

[1] T. Kakuta "Optical Fibers and Their Applications for Radiation Measurements" *Hoshasen* **24[1]** (1998) 41-48 (in Japanese).

[2] T. Oka *et al.* "Development of Fiber Optic Radiation Monitor using Plastic Scintillation fibers" J. Nucl. Sci. Technol. **35[12]** (1998) 857-864.

[3] T. Maekawa *et al.* "Optical Waveguide Scintillator" *Hoshasen* **21[3]** (1995) 69-78 (in Japanese).

[4] S. Koshizuka *et al.* "Researches at the University of Tokyo Fast Neutron Source Reactor, YAYOI." JAERI-M-92-28 (1992) 106-113.

[5] C. Kutsukake *et al.* "Fusion Neutronics. 14MeV Neutron Generation Characteristics of FNS Tritium Target (II). Beam Energy Dependency of Neutron Yield. " JAERI-M-92-125 (1992) 102-104